PERGAMON

Chemical Engineering Science 55 (2000) 1893–1904

Chemical Engineering Science

A new method for estimating hindered creaming/settling velocity of particles in Polydisperse Systems

Sanjeev Kumar[1], Theodore W. Pirog, Doraiswami Ramkrishna*

School of Chemical Engineering, Purdue University, West Lafayette, IN 47907, USA

Received 8 May 1998; accepted 21 June 1999

Abstract

A new experimental technique for measurement of size-dependent settling velocities of particles in polydisperse suspensions (in which particle sizes are distributed continuously) is developed. The new technique employs a continuously fed column, operating at steady state. The size-dependent average hindered velocities of particles present in the column are obtained using the framework of population balances. The proposed technique requires just two measurements of size-specific number densities, one at the inlet to the column and the other at some point in the middle of the column.

The present technique avoids the difficulties with having to observe a multitude of diffused moving fronts in earlier experimental methods, which are also limited to polydisperse suspensions of widely disparate particle sizes. The effects due to multi-body interactions, and surface and inter-particle forces are subsumed by the measurement technique. The technique is also capable of determining velocities of all particles from the dilute limit to the dense over the entire range of polydispersity. Results for many emulsions show good agreement with well-known predictions in the dilute limit. More significantly, substantial deviations in particle speed are measured in dense systems for small particles while the largest particles are accurately represented by the well-known Richardson and Zaki correlation. The technique is capable of measuring the effects of numerous additives, such as glycerin, salts, and gums on creaming dynamics.

Keywords: Velocity; Polydisperse suspensions; Steady state

1. Introduction

Hindered settling (or creaming) of particles in a dense suspension occurs in a large variety of natural and man-made processes. The term "hindered" signifies the constraint on an individual particle from moving "freely" with Stokes velocity (Bird, Stewart & Lightfoot, 1960). The hindrance basically arises from the collective interaction of the particles with the fluid phase (of main interest to hydrodynamicists), and between the particles themselves (of interest to colloid and surface scientists). In describing hindered motion of particles, we actually imply average hindered motion relative to the local volume-averaged fluid velocity, the average being based on both the continuous and the dispersed phase. The averaging process includes both statistical (over all possible particle configurations) as well as spatial averaging such as over a fixed spatial volume. The resulting average hindered velocity is therefore free from variations with position as well as time.

Hindered velocities are crucial to applications in the settling of dispersions, creaming of emulsions and so on. Their theoretical calculation, particularly at high holdup of particles, is belabored by issues connected with inadequate information about inter-particle forces, multi-body interactions, the consequent lack of closure, etc. Determining the hindered velocity from experiment, on the other hand, has been possible only with dispersions that are monodisperse or those that are polydisperse with widely disparate particle sizes. This paper presents a new technique for measuring the hindered settling velocity of particles. The new technique is based on population balance concepts and applies from dilute to dense dispersions without any constraints on the form of polydispersity.

* Corresponding author. Tel.: + 1-765-494-4066; fax: + 1-765-494-0805.

E-mail address: ramkrish@ecn.purdue.edu (D. Ramkrishna)

[1] Present address: Department of Chemical Engineering, Indian Institute of Science, Bangalore 560 012, India

0009-2509/00/$ - see front matter
PII: S0009-2509(99)00457-1

Nomenclature

A	cross-sectional area
d	shear migration factor from Nott and Brady (1994)
D	Diffusivity
g	gravitational acceleration
G	gravity coalescence kernel
n_i, n_e	inlet and exit number densities
$n(v, r, z)$	number density
ϕ	volume fraction
ϕ_i, ϕ_e	inlet and exiting volume fractions
Q	volumetric flow rate
r	radial position
R	column radius
$\Delta\rho$	mass density difference
u_r, u_z	radial and vertical velocity
U_b	average bulk velocity of the fluid
v	particle volume
z	vertical location
$\dot{Z}$	hindered settling velocity

Experimentally, the buoyancy-induced hindered velocity of solid particles in suspensions and hindered velocity of drops in emulsions are obtained in the following manner. A graduated cylinder is filled with the "dispersion" and the "particles" are allowed to settle or cream. To keep the discussion general, and applicable to both suspensions and emulsions, the term "dispersion" will be used; the word "particle" will refer interchangeably to solid particles or drops. For the simple case of dilute to moderately concentrated dispersion of monodisperse particles, an initially homogeneous dispersion evolves into three zones. The first zone consists of clear liquid, the second of dispersion which is the same as the initial one, and the third of sediment or cream. The velocity of the interface separating the clear liquid from the zone consisting of particles is measured and used to obtain the settling velocity of the particles in the second zone (Kynch, 1952). The method has also been extended to obtain hindered velocities of particles in bidisperse and tridisperse systems, provided the particle populations are substantially different from each other in size so that clear interfaces separate various zones and can be monitored for their movement.

In comparison, polydisperse dispersions, the most widely encountered ones in practice, consist of particles lying in a broad size range. The particle sizes are so closely spaced in these dispersions that the particle size space can be considered to be a continuum and the particle population can be represented by a continuous "number density". When a polydisperse dispersion is allowed to settle or cream, it does not give rise to interfaces separating various zones. The conventional methods which rely on tracking of interfaces in a batch column to measure hindered velocities thus fail for polydisperse systems. Furthermore, in settling (or creaming) experiments in a batch column, the relative motion of particles segregates the large particles from the small particle. Hence, the effect of the large particles on the motion of the small ones is not available for direct observation. For these reasons, Batchelor's theory (1982) for hindered motion of particles, which applieds in principle to dilute dispersions, is yet to be tested for truly polydisperse systems.

Another limitation of the conventional method is that even for monodisperse particles, it does not always work. An interface is not a sharply defined plane which can be tracked easily, but rather a diffused region over which particle concentration changes from a finite value to zero. In the presence of small particles, which execute Brownian motion, the region over which particle concentration changes can expand significantly. Therefore, the conventional experimental method can fail for monodisperse particles.

In the present paper, we propose a new experimental method for estimating creaming/settling velocities of particles in polydisperse dispersion. The method naturally applies to both mono and multidisperse (bidisperse, tridisperse, etc.) systems. The proposed method makes use of the framework of population balances and through just two measurements of the size distribution, enables the estimation of hindered velocities of particles lying in a wide size range. The experimental method relies on measuring changes in number density of particles due to their relative motion, rather than monitoring velocities of interfaces. The proposed method thus does not suffer from the limitations of the conventional method discussed before.

The remainder of the paper is organized as follows. In Section 2, we elucidate the principle behind the proposed technique. Section 3 contains the required mathematical justification for an important simplification in the experimental procedure for particle movement under the combined influence of buoyancy and Brownian motion. Section 4 establishes further usefulness of the proposed procedure for large particles which consitute industrially important class of dispersions. The mathematical procedure for obtaining size and environment-dependent settling/creaming velocities from the experimental data is presented in Section 5. Details of the experimental procedure and equipment used are provided in Section 6. The experimental data and a discussion of the proposed experimental technique are presented in Section 7. The experimental data are presented in this paper with a view to only demonstrate the potential of the proposed technique. A detailed analysis of the experimental data for various systems for a variety of experimental

conditions is presented elsewhere (Pirog, Kumar & Ramkrishna, 1999).

2. A new experimental method

Buoyancy-driven relative motion of particles in a dispersion results in segregation of the dispersed phase from the continuous phase. Depending on the application, relative motion of particles may be a desired feature as in thickeners, or an unwanted trouble as in food emulsions. Estimation of particle velocities is, however, necessary to characterize the overall process in all such applications.

In the limit of infinite dilution, the relative velocity between the particle and the fluid is referred to as Stokes velocity in the literature. As the dispersed-phase holdup increases, the hydrodynamic interaction of a reference particle with its neighbors increases and its motion is hindered. Conventionally, the extent of hindering experienced by a particle has been assumed to depend only on the local holdup of particles. Batchelor (1982), in his theory of hindered settling of particles in dilute polydisperse systems, however, shows that the extent of hindering depends on the individual holdups of particles of all sizes that constitute the local environment, and not just their sum total which is the local total holdup. Since Batchelor's theory is limited to binary interactions, it is designed to apply only at suitably low holdup of different sizes.

Before we expound the idea behind the new method proposed in this paper, let us observe that the particle velocities we seek are "mean" quantities obtained by averaging over the local particle configuration. The particle velocities measured here are, however, averaged not only over the local particle configuration but also over the flow cross-section of the column. This constraint of averaging over the cross-section can be overcome by ensuring that the number density is cross-sectionally uniform to a good approximation in order that the measured velocities are only configurationally averaged as required.

Consider a tall vertical column of uniform cross-sectional area, fitted with a conical section, at the bottom for experiments with emulsions and at the top for experiments with suspensions. Suppose that the column is fed with a monodisperse suspension of particles of size v and volume fraction ϕ_{in} at rate Q_{in}. Under steady-state conditions, the volumetric flow of particles at the inlet must match that which comes out, so that, in the absence of diffusion, one must infer the mean hindered velocity of the particles as below.

$$Q_{\text{in}}\phi_{\text{in}} = A[U_b + \dot{Z}]\, nv\,, \tag{1}$$

where A is the cross-sectional area of the column, U_b is the average bulk velocity of the fluid, and n is the number of particles per unit volume in the column. Here, $\dot{Z}$ is the mean hindered velocity of particles with respect to the wall of the container in a non-flowing system at the same number density as in the column. Eq. (1) allows estimation of hindered velocity $\dot{Z}$ as the other quantities appearing in it are either fixed a priori or can be measured experimentally.

For the monodisperse particles considered in this example, nv is the particle holdup in the column and can be measured experimentally. The holdup (or number density) changes in a very small region around the entry point to the conical section of the column. It continues to change further due to the diverging cross-section of the conical section and becomes constant after the column diameters becomes constant.

A generalization of the simplified situation considered above is now undertaken for a polydisperse feed. As the particles of different sizes move with different relative velocities, their concentrations in the column become different from the concentrations at the inlet. By measuring changes in concentration of particles of each size, hindered relative velocity of particles of all sizes present in the column can be determined. When particle sizes are distributed very closely, concentration of particles of various sizes is best represented by a continuous number density. Thus, by measuring changes in number density at the inlet and in the column, the hindered relative velocity of particles present in a polydisperse dispersion can also be determined. By comparing these velocities with the corresponding Stokes velocities, the *size and environment-dependent* hindered creaming correction factor can be obtained in a straightforward way.

The technique can also be used to determine particle velocities in dispersions consisting of particles of different densities. All the particles in the dispersion should however move in the same direction. The estimated size-dependent particle velocities will then correspond to the average velocity of all the particles of various densities but of the same size.

The experimental situation considered thus far, however, encounters a serious operational difficulty — cross-sectional inhomogeneity. The feed to the column is inhomogeneous because of buoyancy-induced segregation in the tube feeding the conical section. Particles attain their terminal velocities in fluid elements moving at different velocities at a given cross section and cause further non-uniformities. Increasing cross-sectional area of the conical section in downstream direction makes the continuous phase move radially. Since the particles move with a net relative velocity along the column axis, expanding cross-section makes particles concentrate in the central region of the column. The particles leaving the conical section are thus distributed non-uniformly. The resulting radial non-uniformities may be accountable in the theory and the measurements, but it will render the proposed technique extremely complex to use.

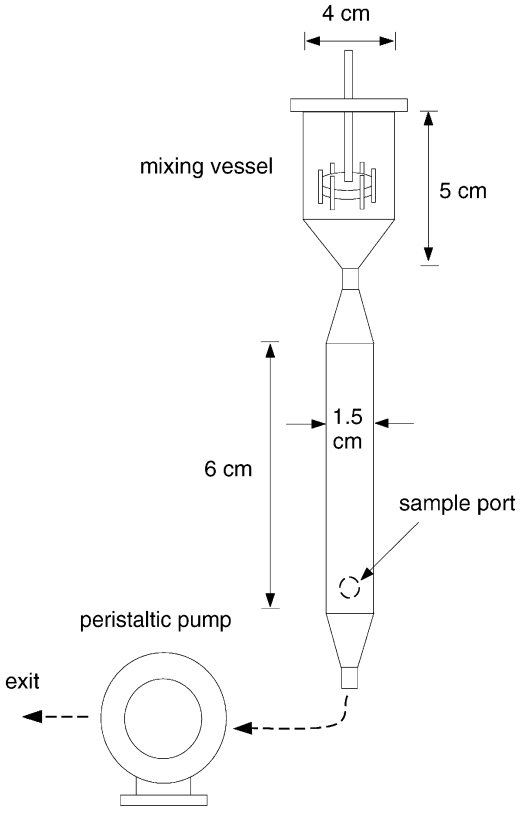

Fig. 1. Experimental setup for settling experiments.

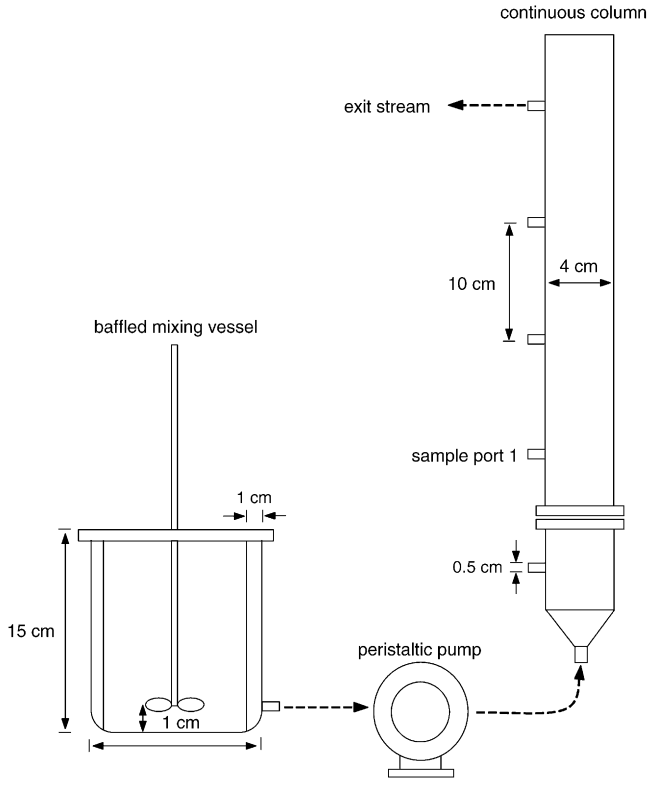

Fig. 2. Experimental setup for creaming experiments.

To keep the new technique simple, the contents of a small segment of column are mixed so that the particles get distributed uniformly at some plane. The setups used to effect it are shown in Figs. 1 and 2.

It is not obvious, however, how the development of a parabolic velocity profile from the irregular velocity profile in the mixer section through the radial component of velocity will not again segregate the particles. Since radial uniformity is essential for the proposed technique, we show that development of velocity profile downstream of the mixer section does not produce any inhomogeneity. We first consider the case of small particles which execute Brownian motion also along with the buoyancy-induced motion.

3. Radial uniformity of particles in presence of particle diffusion

To rigorously establish that the particles mixed in some small segment of the column do not develop any cross-sectional inhomogeneity while the velocity profile changes, we set up continuity equations for both particle and continuous phases for bulk convective motion, relative motion of particles due to buoyancy, and particle diffusion in both radial and axial directions. We assume that $u_r(r, z)$ and $u_x(r, z)$ are local fluid velocities in the radial and axial directions, respectively, and $n(v, r, z)\,\mathrm{d}v$ is the number of particles lying in size range v to $v + \mathrm{d}v$ at physical location (r, z). The relevant balance equation at steady state is

$$\frac{\partial}{\partial z}\left[\{u_z(r,z) + \dot{Z}(v, n(v,r,z))\}\, n(v,r,z)\right] + \frac{1}{r}\frac{\partial}{\partial r}\left(r u_r(r,z) n\right) = \frac{\partial}{\partial z}\left\{D\frac{\partial n(v,r,z)}{\partial z}\right\} + \frac{1}{r}\frac{\partial}{\partial r}\left\{rD\frac{\partial n(v,r,z)}{\partial r}\right\}. \quad (2)$$

The relative velocity of particles of size v, $\dot{Z}(v, n)$, is in contrast with the conventional approaches where $\dot{Z}$ is assumed to depend only on v and ϕ. We consider $\dot{Z}$ to depend on v and local number density n as shown by Batchelor (1982). The above dependence is more general because dependence on ϕ, defined by

$$\phi(r, z) = \int_0^\infty v n(v, r, z)\,\mathrm{d}v \quad (3)$$

can be obtained as a simplified case. The dependence of variables $n(v, r, z)$, $u_z(r, z)$, and $u_r(r, z)$ on v, r, and z has been suppressed in all subsequent equations for notational brevity. A balance similar to Eq. (2) for the continuous phase is

$$\frac{\partial}{\partial z}\{(1-\phi)\,u_z\} + \frac{1}{r}\frac{\partial}{\partial r}\{r(1-\phi)u_r\} = 0\,. \quad (4)$$

Eqs. (2) and (4) can be manipulated to obtain

$$\frac{\partial}{\partial z}\left\{D\frac{\partial n}{\partial z}\right\}+\frac{1}{r}\frac{\partial}{\partial r}\left\{rD\frac{\partial n}{\partial r}\right\}-\{u_z+\dot{Z}(v,n)\}\frac{\partial n}{\partial z}-u_r\frac{\partial n}{\partial r}-\frac{n}{1-\phi}\left[u_r\frac{\partial\phi}{\partial r}+u_z\frac{\partial\phi}{\partial z}\right]=0\,, \tag{5}$$

which is solved with the following boundary conditions:

$$z=0,\ n=n_i(v);\ z\to\infty\,,\ \frac{\partial n}{\partial z}=0\,, \tag{6}$$

$$r=0,\ \frac{\partial n}{\partial r}=0;\ r=R,\ \frac{\partial n}{\partial z}=0\,. \tag{7}$$

To show that non-uniformities do not develop beyond the mixer section, we first assume that ϕ is a constant in Eq. (5) and then validate the assumption a posteriori. Thus, for a constant value of ϕ, we have

$$\frac{\partial}{\partial z}\left\{D\frac{\partial n}{\partial z}\right\}+\frac{1}{r}\frac{\partial}{\partial r}\left\{rD\frac{\partial n}{\partial r}\right\}-\{u_z+\dot{Z}(v,n)\}\frac{\partial n}{\partial z}-u_r\frac{\partial n}{\partial r}=0\,. \tag{8}$$

Defining $\bar{n}(v)=n-n_i(v)$, the above equation can be recast as

$$\frac{\partial}{\partial z}\left\{D\frac{\partial\bar{n}(v)}{\partial z}\right\}+\frac{1}{r}\frac{\partial}{\partial r}\left\{rD\frac{\partial\bar{n}(v)}{\partial r}\right\}-\{u_z+\dot{Z}(v,n(v))\}\frac{\partial\bar{n}(v)}{\partial z}-u_r\frac{\partial\bar{n}(v)}{\partial r}=0 \tag{9}$$

with the following boundary conditions:

$$z=0,\ \bar{n}(v)=0;\ z\to\infty\,,\ \frac{\partial\bar{n}(v)}{\partial z}=0\,, \tag{10}$$

$$r=0,\ \frac{\partial\bar{n}(v)}{\partial r}=0;\ r=R,\ \frac{\partial\bar{n}(v)}{\partial r}=0\,. \tag{11}$$

Using Phragmen–Lindelof principle (Protter and Weinberger, 1967) for unbounded domains, it can be shown that Eq. (9) for arbitrary choices for functions $u_z(z,r)$ and $u_r(z,r)$ and the boundary conditions specified above has only one solution, i.e.,

$$\bar{n}(v)=0$$

or

$$n(v,r,z)=n_i(v)\,.$$

Since $n_i(v)$ is independent of r and z, the assumption made earlier, that $\phi(r,z)$ is a constant, is self-consistent. Thus, once the contents are well mixed artificially in the mixer section, they remain well mixed in the section downstream. The conclusion reached here relies on the presence of the diffusion term in the balance Eq. (2). When the particle size is large, the intensity of Brownian motion decreases. In fact, for particles of radii larger than about 2 μm, the term representing particle diffusion are equated to zero. The next section shows that under these conditions also, non-uniformities do not develop in the section downstream of the mixer section.

4. Radial uniformity of particles

The relevant equation in the absence of particle diffusion can be obtained by dropping the terms corresponding to particle diffusion from Eq. (2). The simpler equation is given as (explicit dependence of various variable on v, r and z has been suppressed for clarity)

$$\frac{\partial}{\partial z}\left[\{u_z+\dot{Z}(v,n)\}n\right]+\frac{1}{r}\frac{\partial}{\partial r}\left[ru_rn\right]=0\,. \tag{12}$$

The balance equation for the continuous phase is the same as Eq. (4). Eqs. (12) and (4) can be combined to obtain

$$\left[\{u_z+\dot{Z}(v,n)\}\frac{\partial n}{\partial z}+u_r\frac{\partial n}{\partial r}\right]+\frac{n}{1-\phi}\left[u_r\frac{\partial\phi}{\partial z}+u_r\frac{\partial\phi}{\partial r}\right]+n\frac{\partial\dot{Z}(v,n)}{\partial z}=0\,. \tag{13}$$

A slight rearrangement of Eq. (13) yields

$$\left[\{u_z+\dot{Z}(v,n)\}\frac{\partial n}{\partial z}+n\left\{\frac{u_z}{1-\phi}\frac{\partial\phi}{\partial z}+\frac{\partial\dot{Z}(v,n)}{\partial z}\right\}\right]+\left[u_r\frac{\partial n}{\partial r}+\frac{n}{1-\phi}u_r\frac{\partial\phi}{\partial r}\right]=0 \tag{14}$$

Eq. (14) provides the basis for establishing radial homogeneity. As before, consider a radial plane at the end of the conical entrance section in which the particles are uniformly distributed. Let us first consider the case of monodisperse particles of volume v_i, i.e., $n(v,r,z)=N_i(r,z)\delta(v-v_i)$, and $\phi=N_iv_i$. Substituting for these in Eq. (14), and replacing $\partial\dot{Z}(v,n)/\partial z$ by $\mathrm{d}\dot{Z}_i/\mathrm{d}\phi\ \partial\phi/\partial z$ yields

$$\left[\{u_z+\dot{Z}_i\}\frac{\partial N_i}{\partial z}+N_i\left\{\frac{1}{1-\phi}u_z+\frac{\mathrm{d}\dot{Z}_i}{\mathrm{d}\phi}\right\}v_i\frac{\partial N_i}{\partial z}\right]+\left[u_r\frac{\partial N_i}{\partial r}+\frac{\phi}{1-\phi}u_r\frac{\partial N_i}{\partial r}\right]=0\,. \tag{15}$$

N_i depends on both r and z here. Rearrangement of the previous equation leads to

$$\left[\{u_z+\dot{Z}_i\}+\phi\left\{\frac{1}{1-\phi}u_z+\frac{\mathrm{d}\dot{Z}_i}{\mathrm{d}\phi}\right\}\right]\times\frac{\partial N_i}{\partial z}+u_r\left[1+\frac{\phi}{1-\phi}\right]\frac{\partial N_i}{\partial r}=0 \tag{16}$$

or

$$\left[\frac{u_z}{1-\phi}+\frac{\mathrm{d}(\phi\dot{Z}_i)}{\mathrm{d}\phi}\right]\frac{\partial N_i}{\partial z}+\left[\frac{u_r}{1-\phi}\right]\frac{\partial N_i}{\partial r}=0\,. \tag{17}$$

Eq. (17) holds for all possible values of u_z. If particles are well mixed in one plane, i.e., $\partial N_i/\partial r$ is zero everywhere in a given plane, Eq. (17) shows that $\partial N_i/\partial z$ will also be identically zero everywhere in this plane. One can now march along the direction of flow and show that particles cannot develop any concentration gradients in a plane a little distance away from the first plane. The argument can be repeated to show that a plane still farther away will also not develop any concentration gradients and so on. Thus, the column, beyond the first well-mixed plane, will be uniform everywhere, excluding the regions near the exit port.

For polydisperse systems, complete radial mixing in a given plane will likewise allow us to drop all radial gradients from Eq. (14). Thus,

$$\{u_z + \dot{Z}(v,n)\}\frac{\partial n}{\partial z} + n\left\{\frac{u_z}{1-\phi}\frac{\partial \phi}{\partial z} + \frac{\partial \dot{Z}(v,n)}{\partial z}\right\} = 0\,. \quad (18)$$

If we assume $\partial \dot{Z}(v,n)/\partial z$ to be zero, the above equation reduces to

$$\{u_z + \dot{Z}(v,n)\}\frac{\partial n}{\partial z} + n\left\{\frac{u_z}{1-\phi}\right\}\frac{\partial \phi}{\partial z} = 0 \quad (19)$$

which shows that in order for the fluid velocity at every point to be in the direction of the average flow, $\partial n/\partial z$ and $\partial \phi/\partial z$ must have opposite signs for all v. Since ϕ is defined as

$$\phi = \int_0^\infty vn\,\mathrm{d}v \quad \text{or} \quad \frac{\partial \phi}{\partial z} = \int_0^\infty v\frac{\partial n}{\partial z}\,\mathrm{d}v\,,$$

the above conclusion can hold only for

$$\frac{\partial \phi}{\partial z} = \frac{\partial n}{\partial z} = 0 \quad \forall v\,. \quad (20)$$

Since,

$$\frac{\partial \dot{Z}(v,n)}{\partial z} = \frac{\mathrm{d}\dot{Z}(v,n)}{\mathrm{d}\phi}\frac{\partial \phi}{\partial z}\,,$$

the assumption $\partial \dot{Z}(v,n)/\partial z = 0$ made in the above analysis is self-consistent.

The arguments presented thus show that uniform distribution in one radial plane ensure that concentration gradients will not develop as the dispersion goes downstream of the mixer section. The presence of shear field because of a net flow through the column may, however, induce some particle migration from high to low shear regions (Gadala-Maria and Acrivos, 1980; Nott and Brady, 1994) and cause non-uniformities in a radial plane.

Nott and Brady (1994) show that the length scale for the effect of shear migration to reach the centerline in pipe flow is given as

$$\frac{L}{D/2} \sim \frac{1}{12d(\phi)}\left(\frac{D/2}{a}\right)^2\,.$$

Here L is the required length, $12d(\phi)$ is approximately 1 for $\phi > 0.3$, D is the tube diameter, and a is the particle radius. Clearly, for a in the range of tens of microns and D being a couple of centimeters, the effect of particle migration can be safely neglected.

Yet another feature of the flowing dispersions which is absent in batch systems is shear-field-induced relative motion and collisions between particles. At low Reynolds number, a reference particle in a constant shear field interacts symmetrically with its neighbors, hence, shear field may not have any net effect on buoyancy-induced relative motion of the reference particle. A non-zero effect is likely only for spatially varying shear field. Flow through the column does produce such a shear field. The effect of shear-field-induced relative motion between particles on the buoyancy-induced relative hindered velocity of particles is not known; however, the effect can be expected to be small if the magnitude of the shear field itself is negligibly small. The smallness of the magnitude of the shear rate can be obtained by estimating the ratio of buoyancy-induced collisions to shear-field-induced collisions. The above ratio for collisions between particles of diameters d_i and d_j, corresponding to the highest shear rate on the wall of the column is given by (see the appendix)

$$\frac{\pi R^3}{24Q}\frac{\Delta\rho g}{\mu}\,|d_i - d_j|\,.$$

For typical values used in experiments, $R = 2$ cm, $Q = 4$ ml/min, $\Delta\rho = 0.1$ g/cm^3, $\mu = 0.01$ P, and $|d_i - d_j| = 2$ μm, the buoyancy-induced collision rate is estimated to be 30 times larger than the shear-field-induced collision rate. Thus, the prevailing shear rates are to small to have any impact. The data presented later suggests that this is indeed valid.

Peysson and Guazzelli (1998) have recently shown that settling of large size monodisperse glass beads (800 μm) in a narrow column (4×4 cm) results in a weak global circulatory flow and introduces non-uniformities in particle concentration across a cross section. The presence of a lighter film near the container wall, because the particle centers cannot enter this film, is the reason for the circulatory flow. The use of the conventional technique to measure particle velocities in such systems will require cross-sectional averages. The present technique can also be used with cross-sectional average number density. However, it is of interest to note that systems having nearly monodisperse particles and very small ratio of column dimension to particle dimension, both of which are required for substantial circulatory flow, are rare. The commonly encountered systems are polydisperse with a large ratio of column dimension to particle dimension and are unlikely to have circulatory flow.

5. The procedure for estimating size-specific creaming velocities

Having established that the number density becomes constant beyond the mixer section, an expression for the relative velocity of the particles can be obtained by balancing the flux of particles entering the column with that passing through a plane located beyond the mixer section. If a dispersion is fed with rate Q and the number density of particles in it is $n_i(v)$, then $Qn_i(v)\,\mathrm{d}v$ is the rate at which particles in size range $(v, v+\mathrm{d}v)$ enter the column. At steady state this rate should equal the rate at which particles are leaving through a plane located beyond the mixer section. Thus, in absence of any concentration gradients,

$$Qn_i(v)\,\mathrm{d}v = \int_0^R \{u_z(r,z) + \dot{Z}(v, n_e(v))\}\, n_e(v)\,\mathrm{d}v\, 2\pi r\,\mathrm{d}r\,, \tag{21}$$

where $n_e(v)$ as the number density beyond the mixed section. Since $n_e(v)$ does not depend on r, the above equation simplifies to

$$Qn_i(v) = n_e(v)\int_0^R \{u_z(r,z) + \dot{Z}(v, n_e(v))\}\, 2\pi r\,\mathrm{d}r\,. \tag{22}$$

A balance for the continuous phase yields

$$Q(1-\phi_i) = \int_0^R u_z(r,z)\,(1-\phi_e)\,2\pi r\,\mathrm{d}r. \tag{23}$$

As ϕ_e is also independent of r,

$$Q(1-\phi_i) = (1-\phi_e)\int_0^R u_z(r,z)\,2\pi r\,\mathrm{d}r\,. \tag{24}$$

Eqs. (22) and (24) can be combined to obtain

$$Qn_i(v) = n_e(v)\left[Q\frac{(1-\phi_i)}{(1-\phi_e)} + \dot{Z}(v, n_e(v))\pi R^2\right] \tag{25}$$

or

$$\dot{Z}(v, n_e(v)) = \frac{Q}{\pi R^2}\left[\frac{n_i(v)}{n_e(v)} - \frac{1-\phi_i}{1-\phi_e}\right]. \tag{26}$$

Thus, given just two measurements of number density, one at the inlet and the other at a location beyond the mixed section but away from the exit port (to avoid end effects), the hindered relative velocities of all the particles at the local environment prevailing there, i.e., $n_e(v)$, can be obtained using Eq. (26). Estimates of ϕ_i and ϕ_e can be obtained from the corresponding number densities using expressions similar to that in Eq. (3).

6. Experimental

Experiments were conducted in a tall vertical column of uniform diameter of 4 cm. The column was equipped with sampling ports located at regular intervals. The sampling ports were closed using a septum through which a needle could be pierced to withdraw samples. The entry to the column consisted of a conical section, expanding from 0.8 cm diameter at one end to the column diameter (4 cm) on the other end over a length of 5 cm. The conical section was located at the bottom of the column for dispersions of lighter particles and at the top for heavier particles. For the latter, the column had to be necessarily filled with the continuous phase before introducing the dispersion. In both cases, feed, which was kept in a well-agitated vessel to ensure constant composition, was pumped into the column using a peristaltic pump. The conical entrance section contained a small magnetic stir bar which was revolved at 50 rpm using rotating magnets outside to ensure complete mixing of particles across the inlet. A schematic of the complete radial mixer is shown in Fig. 3.

The samples of size 300–500 μl were withdrawn for estimation of particle size distribution using needles. The needles were chosen such that their ID was more than ten times the size of largest particle to eliminate the possibility of selective withdrawal of drops. The OD was at least 50 times smaller than the column diameter to minimize disturbance to flow field in the column. The size distributions were measured using a Coulter Counter with a Channelyzer. The Coulter Counter continuously monitors electrical resistance across an orifice. The resistance changes momentarily when a non-conducting particle passes through it; the change in resistance appears as a spike in the signal. The height of a spike is related to the volume of the particle passing through the orifice. Thus, number density as a function of particle volume can be obtained straightaway.

Care was taken to dilute the samples to reduce the holdup inside the Coulter sampling vessel for two reasons. First, high sample concentrations lead to double counting and erroneous number density measurements by the Coulter Counter. Many samples were analyzed at

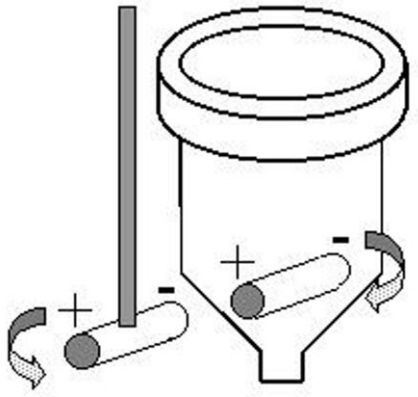

Fig. 3. Magnetic stirrer used to ensure complete radial mixing at column entrance.

various dilutions to ensure reproducible number density measurements and to determine the necessary sample vessel volume fraction to avoid such artifacts. Second, extreme dilution minimizes coalescence of drops. It was verified that surfactants were not necessary to maintain stable particle distributions due to the extremely low volume fraction of samples in the coulter sampling vessel.

The experimental procedure involved suspending the particles in an agitated vessel. For measurement of creaming velocities of drops in emulsions, a fine stable emulsion was first made using Omni lab-scale homogenizer. This emulsion was then kept well mixed in a gently agitated vessel and fed to the column. Samples were taken from the agitated vessel and various ports on the column. The samples from the column ports indicated that the size distribution reached steady state in less than an hour. The measurements also showed that the size distribution did not change as the dispersion moved up in the column to the exit.

Since the estimates of hindered velocity depend on the differences in the size distributions obtained from the agitated vessel and ports in the column, it was thought necessary to ensure that the size distribution did not change due to undesired processes such as drop coalescence, entry effects, etc. Thus, size distributions from the vessel were measured at various times to ensure that the feed to the column did not change with time. The measurements showed that there was no coalescence of drops during the time-scale of the experiment and the feed remained constant. Measurements were also made to ensure that the transport of emulsion from the agitated vessel to the entry point to the column did not change the drop size distribution due to entry effects in the agitated vessel or coalescence of drops during their passage through the connecting tubes. As the samples needed to be kept well mixed in a vessel during the course of its analysis in the Coulter Counter, measurements were made to verify that drops did not undergo coalescence during the measurement time. We found that during the measurement time which was typically about 3 min, no coalescence or dissolution of drops took place. Also, samples taken at different radial positions were identical which establishes radial homogeneity in a plane.

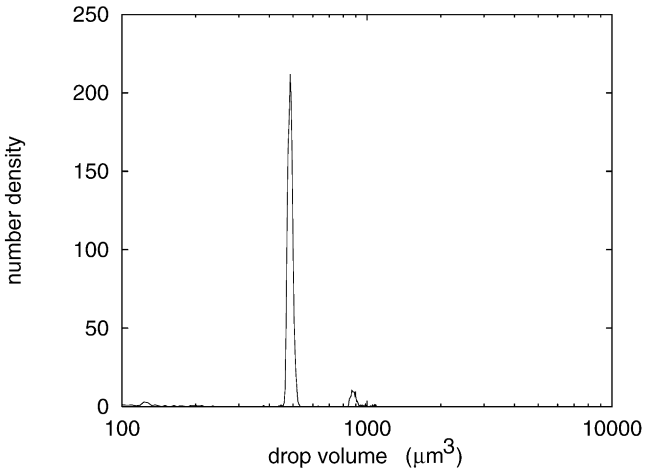

Fig. 4. Number density versus drop volume in the agitated vessel for dilute (0.025% holdup) monodisperse latex particles. The particle diameter is 9.77 μm.

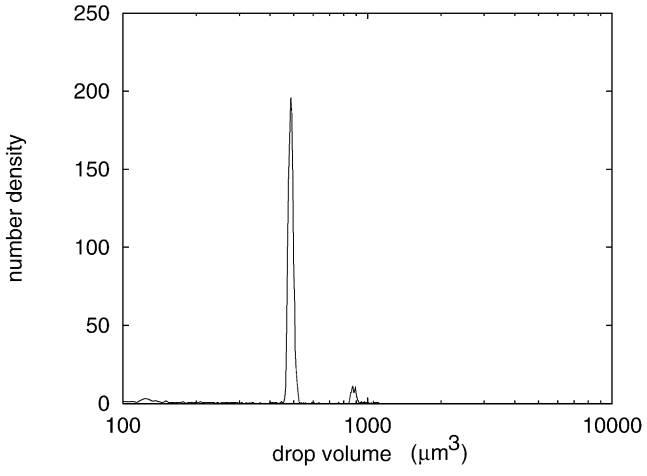

Fig. 5. Number density versus drop volume in the column for dilute monodisperse latex particles. The particle diameter is 9.77 μm.

7. Results and discussion

The new technique needed to be validated first. These experiments were conducted with a suspension of monodisperse latex micro-sphere (diameter = 9.77 μm, density = 1.05 g/ml) at an extremely low holdup (0.025%) at which the settling velocity of particles is expected to be the same as the corresponding Stokes velocity. As the monodisperse latex particles are expensive, a specially designed miniature column (Fig. 1) was used. The number densities at the inlet and at a plane beyond the mixer section were measured at steady state and are shown in Figs. 4 and 5, respectively. The size distributions show that the particles used were almost monodisperse with very little "polydisperse type" interactions. A second small peak in both the figures corresponds to small number of doublets that were present in the sample.

The velocity of monodisperse particles was obtained from the two measurements of number density and Eq. (26) in the following way. The maximum in the measured number density and the corresponding particle volume were taken to represent the nearly monodisperse suspension. Experiments were also performed for monodisperse suspensions of other sizes. At extremely low holdups used in these experiments, the measured velocities are expected to be the same as the corresponding Stokes velocities because the particle–particle interactions are

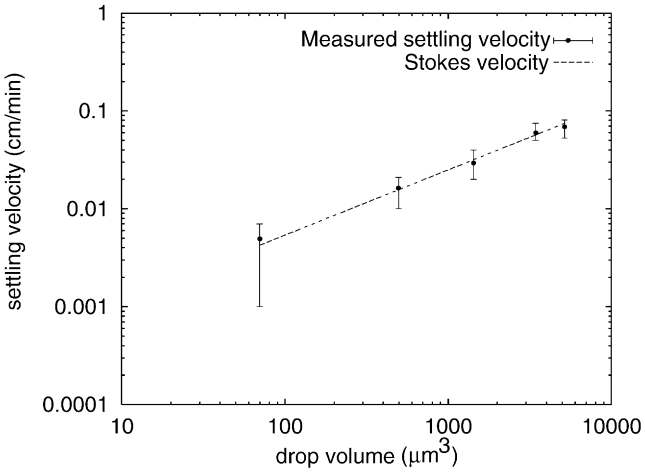

Fig. 6. Settling rates versus drop volume for dilute monodisperse latex particles.

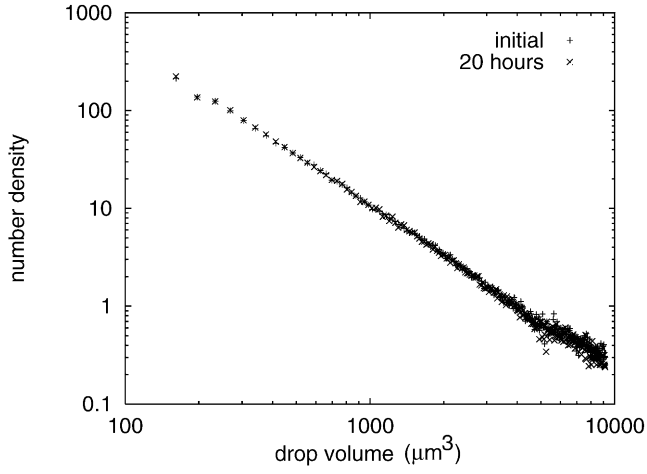

Fig. 8. Number density versus drop volume in agitated vessel for a 1.0% paraffin oil emulsion stabilized with 0.5 wt% SLS.

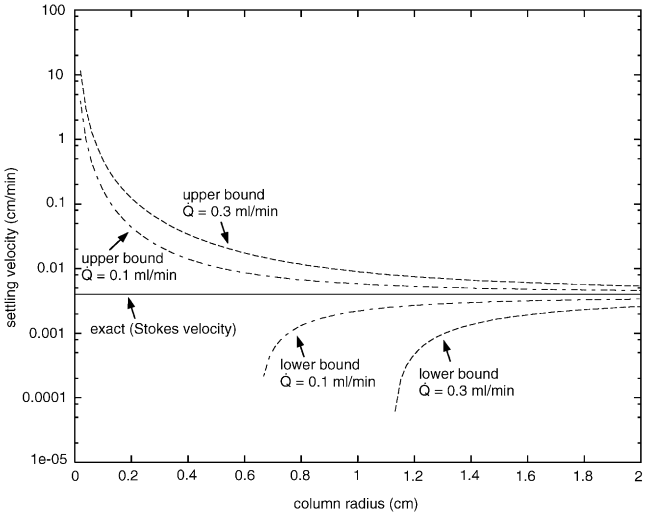

Fig. 7. Error associated with the velocity measurement for a 5 μm latex particle versus column radius. The error bound is given for two flow rates.

nearly zero. Fig. 6 shows that the expected and the measured particle velocities are indeed in good agreement, although with a large error bar for the smallest particles.

While the log-scale exaggerates the error bar for small particles in appearance, the experimental error does become large for small particles. Small particles move with small relative velocities and cause proportionally small difference between the two number densities, making it difficult for the experimental measurements to resolve the difference accurately, hence, the observed increase in the error. The experimental error can be reduced by reducing the bulk flow velocity either by reducing the flow rate or by increasing the column radius. Fig. 7 shows estimated error for 5 μm latex particles as a function of column radius. The error was calculated for 3% error in measurements of number density and 1% error in determination of the flow rate through the column.

Settling of polydisperse particles in batch systems does not give rise to sharp fronts, hence, particle velocities under such conditions could not be measured hitherto. As the focus of the proposed technique is measurement of particle velocities under such conditions, the technique was next tested for extremely dilute polydisperse emulsions. The measured particle velocities under such conditions should correspond to their Stokes velocities. The use of emulsions allowed measurements to be undertaken in a modified tall column assembly shown in Fig. 2. The emulsion system chosen for the experiments was a dispersion of paraffin oil (density = 0.84 g/ml) in 0.5 wt% SLS (sodium lauryl sulfate) solution in water. Surfactant SLS was added to the continuous phase to prevent the coalescence of drops.

Fig. 8 shows the number density in the vessel for 1.0% holdup emulsion at two times: in the beginning of the experiment and much later. The figure shows that as required for the proposed technique, the drop size distribution in the vessel remained constant not just during the course of the experiment ($\sim$ 2 h) but actually much longer than that.

The measured number density in the column displays fluctuations at large particle sizes due to the very small number of particles counted in these size ranges. The size distribution in the column was therefore measured several times to increase the number of large drops counted to reduce fluctuations. Two size distributions, measured at a time interval of 2 h, are shown in Fig. 9. As the data collected at two different times fall on a single curve for the most of the drop size range, steady-state mode of operation is evident. A spatially non-uniform number density in the column indicates coalescence or flocculation of drops. The data for such systems, if used to obtain creaming velocities of drops, will lead to wrong estimates.

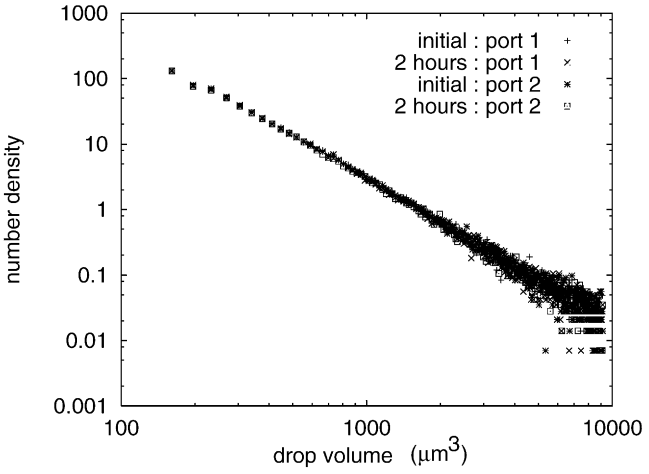

Fig. 9. Number density versus drop volume in column for a 0.2% paraffin oil emulsion stabilized with 0.5 wt% SLS. Identical number densities at two locations in the column establish uniform number density. The scatter for large particle sizes occurs due to their small number.

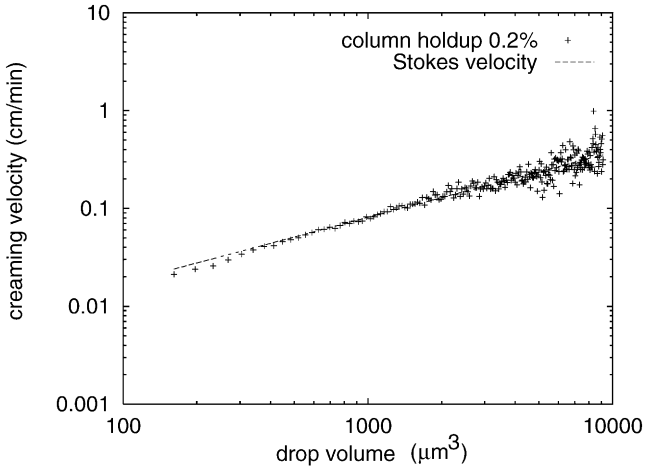

Fig. 10. Creaming rate versus drop volume for a 0.2% paraffin oil emulsion stabilized with 0.5 wt% SLS.

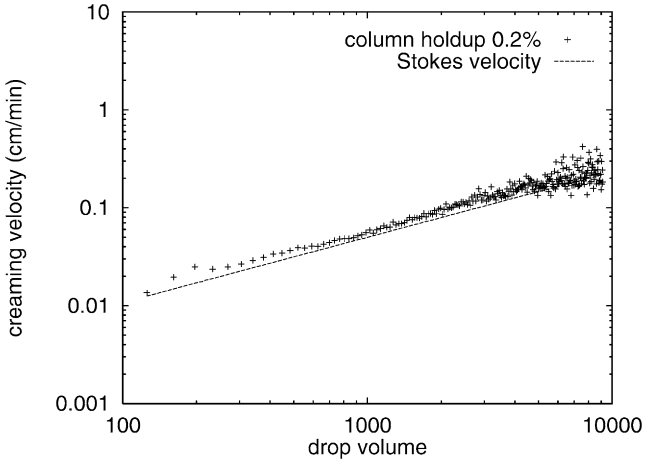

Fig. 11. Creaming rate versus drop volume for a 0.2% soybean oil emulsion stabilized with 0.5 wt% SLS.

To ensure that the drops did not undergo any such undesirable processes, measurements were also made at different ports. The figure shows that all the distributions, measured at different times and different ports, are identical in the size range in which the populations are large and consequently random fluctuations are small.

The size-dependent hindered velocities of drops for the above experiment were obtained using average number densities at the inlet and in the column. The estimated velocities for a holdup of 0.2% in the column are shown in Fig. 10 along with the corresponding Stokes velocities. The good agreement shown in the figure between the measured and the corresponding Stokes velocities establishes the correctness of the proposed technique for polydisperse systems. Thus, if two accurate measurements of number density are available, one at the inlet and the other in the column, the new technique can provide estimates of velocities of drops lying in a broad size range. It is important to point out that the predicted Stokes velocities correspond to spherical solid like drops. This indicates that paraffin oil drops in an emulsion have immobile interface (due to the presence of surfactant on the interface).

To show that the good agreement shown in Fig. 10 is not system dependent, experiments were conducted with another system: soybean oil drops (density = 0.92) dispersed in 0.5 wt% SLS in the aqueous phase. Fig. 11 shows a comparison of the estimated hindered creaming velocities for this system with the corresponding Stokes velocities. The holdup of drops in the mixing vessel and the column were 1.0 and 0.2%, respectively. It is evident from the figure that the proposed technique yields very good estimates for this system as well.

Having demonstrated the ability of the proposed technique to predict the behavior of particles in a polydisperse system at extremely low holdups, we now explore the potential of the present technique to study those systems that could not be studied hitherto because of the limitations of the conventional techniques. These systems are low to high holdup polydisperse dispersions, also the most frequently encountered ones in the industrial practice.

Fig. 12 shows a plot of the measured hindered creaming velocities of drops for a paraffin oil emulsion stabilized with 0.5 wt% SLS. The estimated creaming velocities correspond to a volume fraction of 0.026 in the column, and have been compared with the corresponding Stokes velocities and those obtained by using the correlation of Richardson and Zaki (1954); the latter is meant to describe hindered relative velocity of particles in monodisperse systems, however. As the volume fraction of the dispersed phase in the column is only 0.026, the figure shows that the hindered velocities are predicted to be

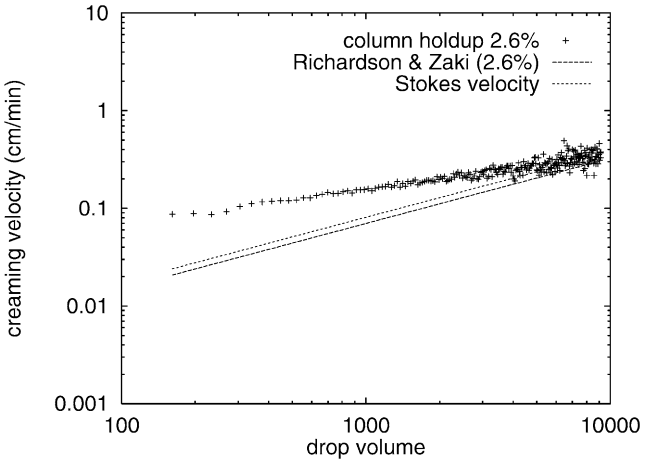

Fig. 12. Creaming rate versus drop volume for a 2.6% paraffin oil emulsion stabilized with 0.5 wt% SLS.

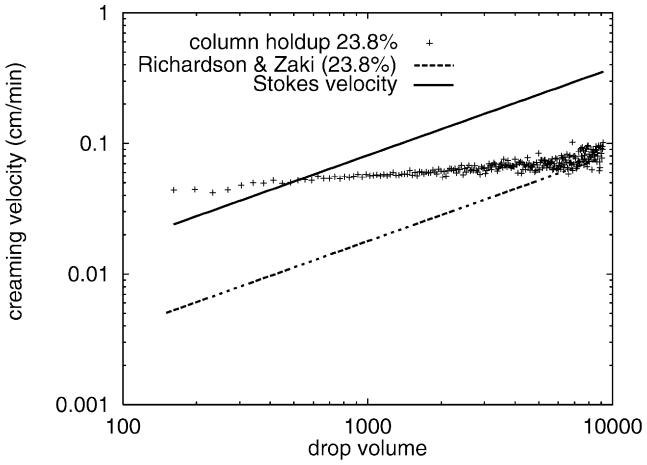

Fig. 13. Creaming rate versus drop volume for a 23.8% paraffin oil emulsion stabilized with 0.5 wt% SLS.

only slightly smaller than the corresponding Stokes velocities. The estimated particle velocities using the new technique, however, show that only the largest drops move with the corresponding Stokes velocities or those predicted using the correlation of Richardson and Zaki (1954). The velocities of the smallest drops, as determined by the experiment, are significantly higher than even the Stokes velocities. The data seem to suggest that the motion of smaller drops is strongly influenced by the presence of the larger drops. The small drops appear to be "dragged" with the larger drops.

To further explore the above possibility, another experiment was conducted for the same system at a moderate holdup of 23.8% in the column. At this holdup, the extent of hindrance to the motion of a drop is predicted to be very large. Fig. 13 shows a comparison of the estimated velocities with the corresponding Stokes velocities and the predictions of the correlation of Richardson and Zaki (1954). The figure shows that the interesting effect of large particles on the motion of the smaller particles is further exaggerated at these holdups. The smaller particles move at almost identical speeds as the large drops; the particle velocities in small size range are in fact larger than the corresponding Stokes velocities. The theory of Batchelor (1982) for polydisperse systems, which predicts particle velocities to be only smaller than the corresponding Stokes velocities because of the hindering effect of other particles present in the system thus appears to be inadequate.

Interestingly, the estimates of drop velocities for both 2.6 and 23.6% holdup show that the correlation of Richardson and Zaki (1954) (which corrects the Stokes velocity assuming a monodisperse system) predicts the large particle movement correctly. This suggests that the motion of large particles is influenced only by the total volume fraction of particles within the system. It is apparent that the influence of the small particles on the large particles is not as significant.

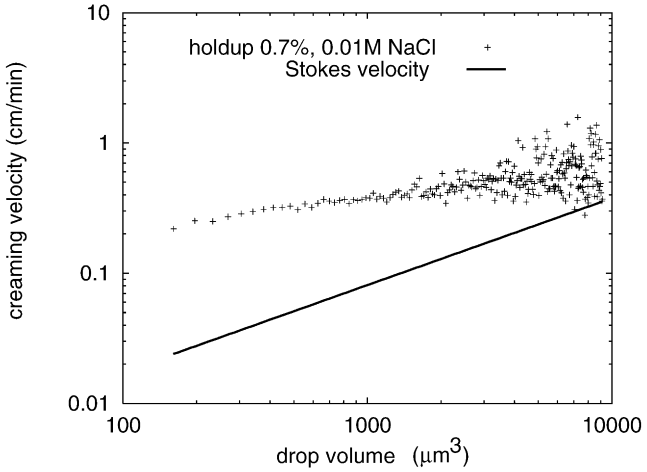

Fig. 14. Creaming rate versus drop volume for a 0.7% paraffin oil emulsion with 0.01 M NaCl stabilized with 1.0 wt% SLS.

Our technique is also capable of measuring the effect of additives on drop–drop interaction potential or the continuous-phase viscosity as changes in these characteristics directly affect the hindered creaming velocity of a particle. The effect of varying drop–drop interaction potential on the measured creaming rate will be illustrated for a paraffin oil emulsion with the addition of an ionic species to alter the droplet–droplet interactions. The hindered creaming velocities of drops for addition of 0.01 M NaCl are shown in Fig. 14 for a column holdup of 0.7%. The figure shows a dramatic increase in the particle velocities compared to the corresponding Stokes velocities. This could be attributed to a reduction in electrostatic repulsion between drops in the presence of screening action of ions. As shown by Batchelor (1982), inter-particle forces can substantially affect the hindered

creaming process in dispersions. Neither the theory leading to Stokes velocity nor the correlation of Richardson and Zaki (1954) accurately predicted the particle velocities. This is to be expected as they do not account for such effects.

8. Summary and conclusions

A new experimental technique to estimate buoyancy-induced hindered velocities of particles/drops in suspensions/emulsions is proposed. The proposed technique can measure particle velocities in monodisperse, polydisperse, dilute and concentrated dispersions. Previous techniques which focused on the moving interface were unable to obtain hindered velocities in polydisperse systems.

The theoretical analysis and the experimental data presented indicate that the technique proposed in this work is quite powerful and robust. Although our analysis in Section 3 shows that diffusion may not affect the results, we have limited ourselves to particle size ranges for which diffusion can be ignored, i.e., for large enough Peclet numbers. An important aspect of the presented technique is the maintenance of cross-sectional uniformity of the particle number density in the column. The technique is capable of estimating particle velocities in a wide variety of systems containing a diverse mixture of different dispersed phases (all heavier or lighter than the external phase), addition of electrolytes, polymers, thickening agents, and many others.

The estimates of drop velocities in polydisperse emulsions, made possible for the first time through the proposed technique, show that the motion of particles changes qualitatively for semi-dilute and dense dispersions when compared to the dilute systems which can be modeled using Stokes velocity. The velocities of small particles in non-dilute dispersions are estimated to be larger than those predicted by the existing theories (Batchelor, 1982) or correlations.

Acknowledgements

The authors thank USDA Grant No. 92-37500-8020 for financial assistance.

Appendix A. Derivation

Buoyancy-induced collision rate:

$$(r_i + r_j)^2 |u_i - u_j| ,$$

where

$$u_i = \frac{2}{9} \frac{\Delta\rho g}{\mu} r_i^2 .$$

Shear-induced collision rate:

$$2\int_0^{\pi/2} 2(r_i + r_j) \sin\theta \mathrm{d}[(r_i + r_j)\cos\theta] G(r_i + r_j)\cos\theta$$

which reduces to

$$(r_i + r_j)^2 \tfrac{2}{3} G(r_i + r_j) .$$

For a given flow rate Q through a pipe of diameter R, the shear rate G at the wall is estimated to be (BSL)

$$G = \frac{4Q}{\pi R^3} .$$

Thus, the ratio of buoyancy- to shear-field-induced collisions comes to be

$$\frac{\pi}{12} \frac{R^3}{Q} \frac{\Delta\rho g}{\mu} |r_i - r_j| .$$

References

Batchelor, G. K. (1982). Sedimentation in a dilute polydisperse system of interacting sphere: Part 1. General theory. *Journal of Fluid Mechanics*, *119*, 372–408.

Bird, R. B., Stewart, W. E., & Lightfoot, E. N. (1960). *Transport Phenomena*. New York: Wiley.

Gadala-Maria, F., & Acrivos, A. (1980). Shear induced structure in a concentrated suspension of solid spheres. *Journal of Rheology*, *24*, 799.

Kynch, G. J. (1952). A theory of sedimentation. *Transactions of the Faraday Society*, *48*, 166–177.

Nott, R. P., & Brady, J. F. (1994). Pressure-driven flow of suspensions: Simulation and theory. *Journal of fluid Mechanics*, *275*, 157–199.

Peysson, Y., & Guazzelli, E. (1988). An experimental investigation of the intrinsic convection in a sedimenting suspension. *The Physics of Fluids*, *10*, 44–54.

Pirog, T. W., Kumar, S. G., & Ramkrishna, D. (1999). On the hindered motion of particles in dense polydisperse suspensions, in preparation.

Protter, M. H., & Weinberger, H. F. (1967). *Maximum principles in differential equations*. Englewood Cliffs, NJ: Prentice-Hall.

Richardson, J. F., & Zaki, W. N. (1954). Sedimentation and fluidisation: Part 1. *Transactions of the Institution of Chemical Engineers*, *32*, 35–53.